Available online at www.sciencedirect.com
SCIENCE DIRECT®
Physics of the Earth and Planetary Interiors 149 (2005) 65–79
PHYSICS OF THE EARTH AND PLANETARY INTERIORS
www.elsevier.com/locate/pepi

Subduction-related intermediate-depth and deep seismicity in Italy: insights from thermal and rheological modelling

E. Carminati [a, b, *], A.M. Negredo [c], J.L. Valera [c], C. Doglioni [a]

[a] *Dipartimento di Scienze della Terra, Universita' degli Studi di Roma "La Sapienza", P.le Aldo Moro 5, I-00185 Roma, Italy*
[b] *Istituto di Geologia Ambientale e Geoingegneria, CNR, P.le A. Moro 5, I-00185 Roma, Italy*
[c] *Department of Geophysics. Faculty of Physics, University Complutense of Madrid, Spain*

Received 30 July 2003; received in revised form 23 January 2004; accepted 26 August 2004

Abstract

Geological data suggest that, after a period of oceanic lithosphere subduction, about 170 km of continental lithosphere were subducted under the Northern Apennines since about 23 Myear at rates of ca. 1 cm/year, whereas more than 700 km of Mesozoic oceanic lithosphere (Ionian lithosphere) have been subducted under the Calabrian arc at rates of about 3 cm/year. However, a well-developed Wadati-Benioff zone can be only recognised below the Calabrian arc down to depths of 450–500 km, whereas intermediate-depth seismicity reaches maximum depths of about 90 km under the Northern Apennines.

We model the thermal state of these two subduction zones and apply temperature-dependent non-linear rheological laws to evaluate the down-dip extent of brittle regions in the two subduction zones. We show that differences in subduction rate and in slab composition (continental vs. oceanic) produce a far deeper (down to 290–380 km) brittle field in the colder Calabrian slab than in the warmer Northern Apenninic slab (70–120 km), thus explaining differences in the maximum depth of seismicity in both regions.

Concerning deep earthquakes in the Calabrian subduction zone, models predict that metastable olivine persists down to depths of 430 km. This could possibly explain the maximum depth of earthquakes in the area. The small extent of the metastable olivine wedge produces a small density anomaly that cannot explain the pervasive down-dip compression observed in the Ionian slab.
© 2004 Elsevier B.V. All rights reserved.

Keywords: Oceanic and continental subduction; Intermediate and deep seismicity; Rheology; Temperature

1. Introduction

The tertiary to present (last 23 Myear) evolution of the central Mediterranean region (Fig. 1) is primarily controlled by the eastward–southeastward rollback of a slab subducting towards the west under the Apennines belt (e.g., Malinverno and Ryan, 1986). In this area, continental and oceanic subductions occur under

* Corresponding author. Tel.: +39 06 49914950; fax: +39 06 4454729.
E-mail address: eugenio.carminati@uniroma1.it (E. Carminati).

0031-9201/$ – see front matter © 2004 Elsevier B.V. All rights reserved.
doi:10.1016/j.pepi.2004.04.006

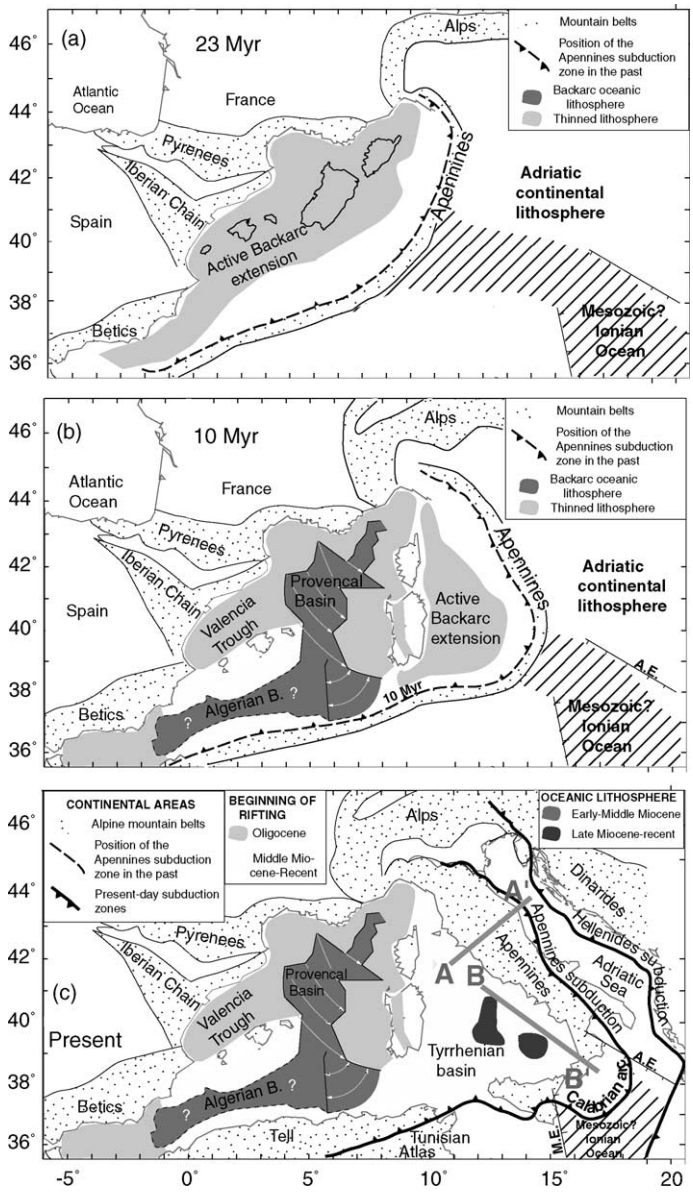

Fig. 1. Sketch of the Tertiary geodynamic evolution of the central and western Mediterranean area. Notice the eastward migration of the Apennines subduction zone in the last 23 Myear. The position of the subduction zone at 23 and 10 Myear is after Gueguen et al. (1998). The geometry of the Provencal Basin is after Burrus (1984) and Bayer et al. (1973). M.E.: Malta Escarpment; A.E.: Apulia Escarpment.

the Northern Apennines and the Calabrian arc respectively (e.g., Gueguen et al., 1998). This peculiar character allows us to study the control of the nature (either continental or oceanic) of subducting slabs on the distribution of subduction-related seismicity. In particular we aim at explaining why the subcrustal seismicity of the area (Fig. 2) does not univocally and clearly indicate the existence of a continuous and deep slab under the entire Apennines-Calabrian arc. In fact, a well-developed Wadati-Benioff plane is imaged below the Calabrian arc down to depths of 450–500 km (Giardini and Velonà, 1991; Frepoli et al., 1996). In contrast, sub-

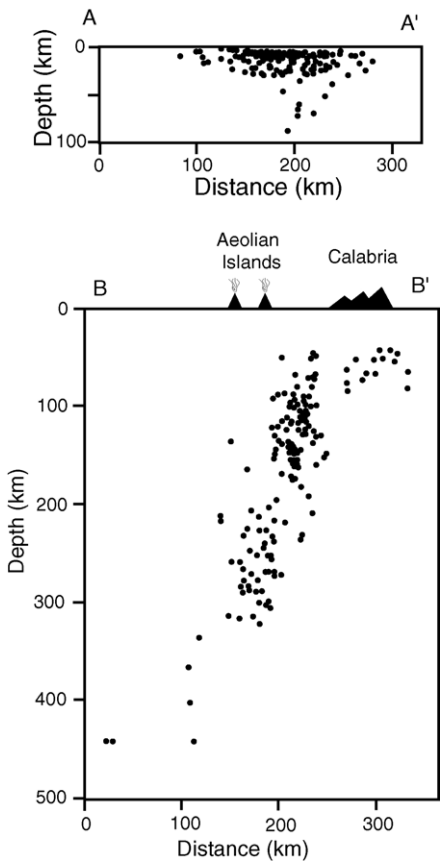

Fig. 2. Seismic distribution along two sections through the Northern Apennines (A–A′; data after Amato and Selvaggi, 1991) and the Calabrian Arc (B–B′; data after Frepoli et al., 1996). The traces of the sections are represented in Fig. 1.

crustal seismicity reaches maximum depths of about 90 km in the Northern Apennines (Amato et al., 1993). As previously suggested by Carminati et al. (2002), we show that the absence of seismicity deeper than 90 km under the Northern Apennines is not the direct evidence for the absence of a slab. It rather could in part be related to the different nature (continental vs. oceanic) of the subducting slabs.

A factor that further increases the complexity of the central Mediterranean is that average Tertiary-Present rollback rates, and therefore subduction rates, increase from north to south (from less than 1 cm/year to more than 3 cm/year; Gueguen et al., 1998). We show that the thermal structure of the subducting slab, which is mainly controlled by subduction rate and thermal state of the lithosphere prior to subduction, changes radically from north to south and strongly controls the geometry of the region where brittle failure causing earthquakes can occur.

These goals are achieved by modeling the thermal structure of the Northern Apennines and Calabrian subduction zones and using temperature-dependent nonlinear rheological laws to determine the prevailing, either ductile or brittle, deformation mechanisms. Modeling results are compared with available seismicity data. Finally, we briefly discuss the origin of the deep (depth greater than 350 km) seismicity of the Calabrian subduction zone.

2. Tertiary tectonic evolution

The Apennines (Fig. 1) are a Late Oligocene to present mountain belt, related to the “west”-directed subduction of the Adriatic plate under the European plate (e.g., Carminati et al., 1998; Doglioni et al., 1999). At the subduction trench, the sedimentary cover of the subducting Adriatic plate is offscraped and accreted into the Apennines belt. The Apennines wedge is an east-vergent thin-skinned fold-and-thrust belt with a foredeep basin at its front. Both the active compressional wedge and the foredeep basin migrated eastward from the Late Oligocene to the Present (e.g., Ricci Lucchi, 1986; Vai, 1989; Patacca and Scandone, 1989). To the west, the Apennines are dissected by the Tyrrhenian and Tuscan extensional basins, interpreted as back-arc basins that developed since the Tortonian (Bigi et al., 1990; Patacca and Scandone, 1989). The volcanic systems (Late Miocene to recent) of the Tuscany, Latium and Campania provinces and of the Eolian Islands are interpreted as a forming volcanic arc (e.g., Serri et al., 1993). The compression-extension couple and the magmatism show eastward migration through time. This has been interpreted as the effect of the eastward to southeastward rollback of the hinge of the west directed subduction (e.g., Malinverno and Ryan, 1986; Gueguen et al., 1998; Carminati et al., 1998), in a regime of no east-west convergence.

The characters of the downgoing plate change from north to south: (i) thinned continental lithosphere subducts in the north (along the Adriatic Sea) and the southwest (Sicily and Sicily channel); (ii) oceanic lithosphere (Ionian lithosphere) subducts under the Cal-

abrian arc. The nature of the lithosphere subducted in the past under the Apennines can be inferred from the analysis of the sediments offscraped from the slab and cropping out in the Apennines.

In the Northern Apennines, the retro-deformation of the orogenic wedge shows that the sediments forming the Apennines were deposited on stretched continental lithosphere and that their east-west extent was close to about 170 km (e.g., Bally et al., 1986). As a consequence, after a period of oceanic lithosphere subduction, about 170 km of continental lithosphere were subducted under the Northern Apennines. The continental nature of the subducting Adriatic plate is confirmed by geochemical and petrological studies on the Neogene-Quaternary magmatism of central Italy (Serri et al., 1993). The thinned Adriatic continental lithosphere in the foreland of the Northern Apennines is about 70 km thick (Calcagnile and Panza, 1981).

Seismic reflection profiles and geological studies show that the Northern Apennines belt is composed almost exclusively of sediments which were offscraped (thin-skinned tectonics) from the subducting Adriatic plate (Bally et al., 1986). No basement rocks (i.e., crystalline crustal rocks) or no more than a few km-thick slices were therefore scraped off from the subducting slab and accreted to the Apennines fold-and-thrust belt. Although quite peculiar when compared to other continental subduction zones, this implies that the continental crust was almost completely subducted with the lithospheric mantle.

The amount of eastward migration of the Northern Apenninic arc—equal to the amount of subduction and of subduction hinge retreat (since convergence is null)—is about 200–250 km in ca. 23 Myear (Boccaletti et al., 1990a; Boccaletti et al., 1990b; Gueguen et al., 1998; Doglioni et al., 1999; Fig. 1). This suggests average subduction rates of about 1 cm/year. The length of the lithosphere subducted under both the Northern Apennines and the Calabrian arc (see below) was evaluated using four data sets: (i) seismic tomography profiles; (ii) migration of backarc extension; (iii) migration of subduction related magmatism; (iv) migration of compressional deformation and of associated foredeep deposits. The errors for both subduction zones can be constrained to some 10–15% of the preferred values.

Subduction rates decrease toward the north and increase to the south. The maximum amount of the deformation front retreat (about 775 km during the last 23 Myear) occurred in the Calabrian arc (Gueguen et al., 1998; Doglioni et al., 1999; Fig. 1). This estimate constrains subduction rates at about 3–3.5 cm/year along the Calabrian arc. The present-day Ionian basin, subducting under the Calabrian arc, is most likely a remnant of Mesozoic oceanic lithosphere. The interpretation of its oceanic nature is mainly based on stratigraphic (Biju-Duval et al., 1982; Catalano et al., 2001) and geophysical data (e.g., Della Vedova and Pellis, 1989; de Voogd et al., 1992; Catalano et al., 2001). The oceanic subduction under Calabria is consistent with the geochemistry of the calcalcaline magmatism of the Aeolian volcanic arc (Barberi et al., 1973). Unlike the Northern and Southern Apennines, the westward subduction that occurred in the last 23 Myear under Calabria did not complete the consumption of the Tethyan oceanic lithosphere. Along this tract of the arc, therefore, no continental subduction has occurred. As far as the age of the subducted oceanic lithosphere is concerned, no precise ages are available. Based on the low values of heat flow densities (30–40 mW m^{-2}), Della Vedova and Pellis (1989) proposed a Mesozoic age (180–200 Myear) for the oceanic lithosphere.

3. Subcrustal seimicity of Italy

Only two regions of Italy are characterized by earthquakes at depths greater than 40 km: the Northern Apennines and the Southern Tyrrhenian Sea (Fig. 1). In the Northern Apennines region (Fig. 2a), the seismicity distribution defines the geometry of the Adriatic continental slab down to 90 km. The slab dips, at 40–90 km depths, about 45° to the west (Amato et al., 1997). Seismic tomography shows, under the Northern Apennines, a high velocity body reaching depths of at least 250 km with ca 60° dip at 100–250 km depths (Amato et al., 1993; Piromallo and Morelli, 1998).

The Calabrian subduction zone (Fig. 2b) is the region of Italy with the highest seismic energy release (Amato et al., 1997). Tens of intermediate (for our purposes, at depths between 40 and 350 km) and deep earthquakes (depths greater than 350 km) per-year are recorded. These earthquakes define a well-developed Wadati-Benioff zone (e.g., Caputo et al., 1970; Giardini and Velonà, 1991). Below 100 km depth the Ionian slab dips at least 70° (Frepoli et al., 1996). The maximum

frequency of earthquakes occurs in the 200–350 km depth interval. Seismic tomography models agree in imaging a fast velocity anomaly down to ca. 500 km, in correspondence with the Wadati-Benioff zone (e.g., Amato et al., 1993; Spakman et al., 1993; Piromallo and Morelli, 1998; Lucente et al., 1999). Spakman et al. (1993) imaged an interruption of the Ionian slab at about 150 km depth, interpreted as a slab detachment. Later models, however, did not confirm the existence of this feature (Piromallo and Morelli, 1998 and Piromallo and Morelli, 2002; Lucente et al., 1999). At depths deeper than 500 km, the aseismic Ionian slab seems to deflect and flatten on the 670 km discontinuity (Lucente et al., 1999; Piromallo and Morelli, 2002). Reliable fault plane solutions of major earthquakes show an overall pervasive down-dip compressional state of the Ionian slab (Isacks and Molnar, 1971; Anderson and Jackson, 1987; Giardini and Velonà, 1991; Frepoli et al., 1996).

4. Thermo-kinematic and rheological modelling

The temperature distribution within the slab and surrounding mantle is calculated using the TEMSPOL code (Negredo et al., 2004). This code permits the calculation of temperature and density anomaly distributions in deep subduction zones, taking into account self-consistently the olivine to spinel phase transformation. The code adopts a finite difference scheme to solve the heat transfer equation

$$\left(1+\frac{L_\mathrm{T}}{C_\mathrm{p}}\frac{\partial\beta}{\partial T}\right)\left(\frac{\partial T}{\partial t}+v_x\frac{\partial T}{\partial x}+v_z\frac{\partial T}{\partial z}\right) = \frac{K}{\rho c_\mathrm{p}}\left(\frac{\partial^2 T}{\partial x^2}+\frac{\partial^2 T}{\partial z^2}\right)-v_z\left(\frac{\alpha g}{c_\mathrm{p}}T_\mathrm{abs}+\frac{L_\mathrm{T}}{c_\mathrm{p}}\frac{\partial\beta}{\partial z}\right)+\frac{H+A_\mathrm{sh}}{\rho c_\mathrm{p}} \quad (1)$$

where L_T is the latent heat due to the olivine-spinel transformation, c_p is the heat capacity, β is the fraction of spinel, T is the temperature, t is time, x and z are the coordinates, v_x and v_z are the horizontal and vertical components of the velocity, K is the thermal conductivity, ρ is the density, α is the coefficient of thermal expansion, g is the acceleration of gravity, T_abs is the absolute temperature, H is the radiogenic heat production rate, and A_sh is the shear heating rate. The values of the parameters used are listed in Table 1.

Table 1
Common parameters used in the thermal model

Thermal parameter	Value
Thermal conductivity	$3.2\,\mathrm{W\,m^{-1}\,K^{-1}}$
Specific heat	$1.3\times10^{3}\,\mathrm{J\,K^{-1}\,kg^{-1}}$
Thermal expansion coefficient	$3.7\times10^{-5}\,\mathrm{K^{-1}}$
Density of the lithospheric mantle at T = 0 °C	$3400\,\mathrm{kg\,m^{-3}}$
Density change due to ol-sp phase transition	$181\,\mathrm{kg\,m^{-3}}$
Lithospheric thickness	Variable
Temperature at the base of the lithosphere	1450 °C
Subduction dip angle	Variable

The terms on the left side represent the rate of heat change due to the temperature change at a fixed point and advection. The first term on the right side represents heat conduction. The term containing T_abs describes the adiabatic heating. The term containing L_T represents the latent heat of the olivine to spinel transformation, and the last term accounts for radiogenic and dissipative heating. The initial thermal distribution of the oceanic lithosphere is calculated with the thermal plate model GDHI of Stein and Stein (1992). The code also includes the possibility of simulating continental subduction, with an initial geotherm for the crust and lithospheric mantle given by the steady-state solution of the heat conduction equation. We assume an adiabatic initial temperature profile for the asthenosphere. We also include a total temperature increase of ΔT, caused by the latent heat released during the olivine to spinel phase change, which initiates at z_{tr2} and is completed at z_{tr1} (see Fig. 3). In this interval the temperature increase is given by (Turcotte and Schubert, 2002)

$$\Delta T = \frac{L_\mathrm{T}}{c_\mathrm{p}}$$

We have followed the approach described by Schmeling et al. (1999) of adopting a simplified phase diagram (from original data by Akaogi et al., 1989 and Rubie and Ross, 1994) to compute the fraction of spinel (β) and its derivatives at any temperature and depth.

The code TEMSPOL also computes the lateral anomaly of density (with respect to an unperturbed col-

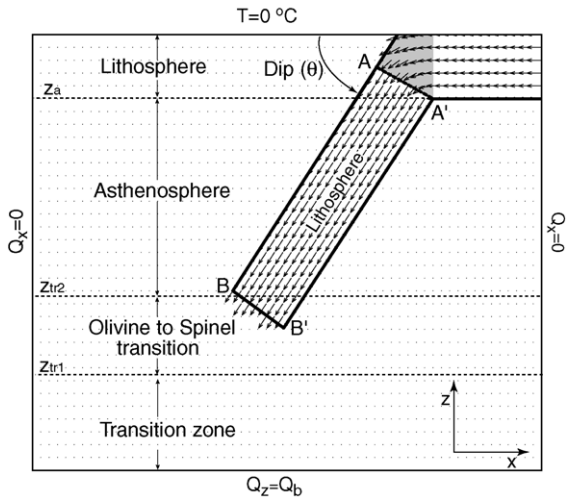

Fig. 3. Schematic diagram illustrating the model domain and applied boundary conditions. Small points indicate nodes of the finite difference grid. The velocity field imposed to simulate subduction is updated as the slab penetrates into the surrounding mantle (modified after Negredo et al., 2004).

umn) due to thermal expansion and phase changes. No density changes induced by high pressure–low temperature metamorphism are taken into account.

In our thermo-kinematic approach the velocity field (Fig. 3) is imposed and defined by the subduction velocity v_s and the slab dip θ. Our modelling procedure shares many characteristics with the thermal model by Minear and Toksöz (1970). The velocity field is updated as the slab penetrates into a static mantle. At each time step, the position (B–B′ in Fig. 3) of the bottom edge of the slab (which was located along A–A' at $t = 0$) is computed, and the slab velocity field is applied to the nodes reached by line B–B′.

We have applied the alternating direction implicit (ADI) method for the finite difference formulation of the energy equation (Eq. (1)). The resulting equations are solved by applying the Thomas algorithm. Provided that the numerical scheme applied is not stable for every combination of vertical, horizontal and time increments, the last one is internally computed by the code to ensure stability. The reader is referred to Negredo et al. (2004) for further details about modelling procedure, numerical method and TEMSPOL code availability.

The geometric and kinematic parameters adopted in the modelling are consistent with the geological and geophysical data described in the previous sections. The thermal parameters are indicated in Table 1. The thermal modelling of the subduction zone under the Northern Apennines assumes a 70 km thick continental slab dipping 60°. We consider heat production for a 20 km thick continental crust. The assumption of 20 km of subducting continental lithosphere is compatible with the thin-skinned tectonics (see the previous section) which characterises the Apennines belt. The Calabrian subduction zone is modelled simulating a 95 km thick oceanic slab with a 70° dip and an age of 120 Myear. A crustal thickness of 10 km and no radioactive heat production is assumed for the oceanic crust. A sensitivity analysis on the effects of varying the age of the subducting oceanic lithosphere between 90 and 150 Myear has been performed. This analysis reveals that results remain almost the same, since the thermal state of the subducting plate does not change significantly within this range of ages.

The thermal and reological modelling consists in the following steps. First, the present day thermal fields of the Northern Apennines and Calabrian subduction zones are obtained using the TEMPSPOL code. Then, the brittle and ductile rheological laws discussed in the following section are imposed a posteriori to infer the behaviour of different sectors of the slabs. In particular, for each node of the finite difference grid, the brittle and ductile strengths are calculated in order to predict whether deformation is more likely to be accommodated by frictional sliding and fracturing or by ductile creep.

4.1. Rheological modelling

Down to depths of about 200–300 km, subcrustal seismicity within subducting slabs is likely to be accommodated by rupture within the brittle field (e.g., Green, 1994). This idea is supported by the observation that the frequency of earthquakes in subducting slabs declines down to 300 km (Kirby et al., 1991). The frequency of earthquakes increases again below 300 km. These deeper earthquakes are generally related to other mechanisms, such as transformational faulting (Green et al., 1990; Kirby et al., 1991 and Kirby et al., 1996) or plastic instabilities (Ogawa, 1987; Hobbs and Ord, 1988).

After the early report in the 1920s of earthquakes occurred at depths greater than 200 km, Jeffreys (1929) pointed out that fracture and frictional strengths in-

crease with depth. As a consequence, the shear stresses necessary to produce brittle faulting at several hundred kilometers depth were considered too high. To solve this critical point, dehydration processes of crustal and mantle minerals were proposed to enhance brittle fracture and frictional sliding (dehydration embrittlement) at depths between 50 and 300 km (e.g., Raleigh and Paterson, 1965; Meade and Jeanloz, 1991; Kirby et al., 1996). A good evidence for dehydration embrittlement is the correlation between the distribution of intermediate-depth seismicity and locations of hydrous minerals predicted by thermal-petrologic models (e.g., Wang, 2002; Hacker et al., 2003; Yamasaki and Seno, 2003).

We first concentrate on intermediate-depth earthquakes (40–350 km) of the Italian area, investigating whether temperature (slow versus fast subduction) and rheological (continental versus oceanic subduction) differences can explain: (i) the absence of earthquakes deeper than 90 km where the continental Adriatic plate slowly (ca. 1 cm/year) subducts under the Northern Apennines; (ii) the existence of a continuous Wadati–Benioff zone within the faster (3 cm/year) subducting Ionian oceanic slab. Once the temperature distribution is obtained using the TEMPSPOL code, we compute at each grid node the brittle and ductile yield stress imposing a posteriori the rheological laws.

In agreement with previous rheological studies, we use the Sibson's law (Sibson, 1981) to calculate the brittle yield stress (differential stress, $\sigma_1 - \sigma_2$). This law, based on the Coulomb–Navier frictional criterion, predicts a linear increase with depth of the yield stress:

$$\sigma_1 - \sigma_3 = \beta\rho g z(1 - \lambda) \quad (2)$$

where β is a parameter depending on the fault type, ρ is the density, g is the gravity acceleration, z is the depth and λ is the pore fluid pressure ratio (i.e., the ratio between fluid pressure and lithostatic load). In our calculations, the β parameter is assumed as 3 (compressional earthquakes predominates at shallow depth within slabs) and the average density $\rho = 3200\ \mathrm{kg\ m^{-3}}$. The fluid pressure is the least constrained parameter of the Sibson's law. We therefore evaluate the effects of changing this parameter. A first reasonable assumption that we consider (brittle strength distribution B1 in Fig. 4) is that fluid pressure is hydrostatic ($\lambda = 0.4$). Several studies suggest that intermediate earthquakes

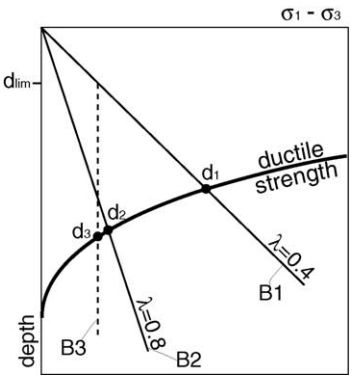

Fig. 4. Qualitative rheological profile showing a curve of ductile strength (referred for example to Olivine) and three different curves (lighter lines) of brittle strength: (i) Sibson's law for $\lambda = 0.4$; (ii) Sibson's law for $\lambda = 0.8$; (iii) Sibson's law down to depth $\mathrm{dli_m}$ and constant brittle strength to deeper depths. Considering the three different brittle strength distributions, three brittle-ductile transition depths (d1–d3) occur.

could be related to embrittlement induced by dehydration of slab minerals (e.g., Raleigh and Paterson, 1965; Meade and Jeanloz, 1991; Wang, 2002). Dehydration processes, due to metamorphic reactions, produce fluid pressures greater than lithostatic pressures (i.e., $\lambda > 0.4$). Such fluid overpressures are thought to reduce the brittle strength and increase the down-dip extent of brittle areas in subducting slabs. To evaluate the effects of fluid overpressures we run models with a brittle strength distribution (B2 in Fig. 4) calculated from the Sibson's law (parameters as before) with $\lambda = 0.8$.

However, the applicability of the Coulomb-Navier criterion has been confirmed experimentally only down to mid-crustal depths (Byerlee, 1978; Jaeger and Cook, 1979). Extrapolating it at higher depths could result in unrealistically high brittle strength. This observation is consistent with the experimental evidence that the coefficient of friction decreases with increasing confining pressure (Jaeger and Cook, 1979). Moreover, experiments on rock mechanics evidenced that high-pressure fracture mechanisms substitute, at depth, frictional failure (Shimada, 1993). These mechanisms are weakly dependent on pressure (Ranalli, 1997). Fracturing experiments on granites show that, at high pressures, the brittle strength becomes approximately constant (Shimada, 1993). Granites can sustain maximum differential stresses ($\sigma_1 - \sigma_3$) of about 200 MPa

(Shimada, 1993). Lithospheric mantle rocks are likely to support higher differential stresses (Ranalli, 1997; Fernandez and Ranalli, 1997). Maximum strength of about 500 MPa can be reasonably assumed for such mantle rocks.

For these reasons, we test a third distribution (B3) of brittle strength with depth (Fig. 4), consistent with the considerations above. We use the Sibson's law at depths shallower than 10 km (parameters as before). Fluid pressure is assumed hydrostatic ($\lambda = 0.4$), consistently with analyses of in situ stress measurements at crustal levels. At depths deeper than 10 km the brittle yield stress is kept constant and equal to that calculated with the Sibson's law at 10 km depth. The maximum yield stress (at 10 km depth) is of about 480 MPa, compatible with the experimental values outlined above.

The three brittle strength distributions at depth (B1 to B3) will result in three different brittle-ductile transition depths (d_1 to d_3), as shown in Fig. 4. Both B2 and B3 strength distributions reduce the brittle strength at depth and therefore tend to increase the brittle-ductile transition depth.

For the ductile behaviour we adopt the following power law creep relation,

$$\sigma_1 - \sigma_3 = \left(\frac{\dot{\varepsilon}}{A}\right)^{1/n} \exp\left(\frac{Q}{nRT}\right) \quad (3)$$

where $\dot{\varepsilon}$ is the effective strain rate, A is the generalised viscosity coefficient, n is the stress power law exponent, Q is the activation energy, R is the gas constant and T is the absolute temperature.

For simplicity we assume a strain rate value constant throughout the model domain, so that we are computing resistance opposed to deformation with a fixed strain rate. In our purely kinematic approach the velocity field is prescribed. Therefore, this kind of modeling does not allow for a feedback on the flow structure within the slab and does not compute the distribution of strain rate. So we neglect the occurrence of local variations of the strain rate, which are likely to occur in subducting slabs. However, we check the sensitivity of the models to this parameter varying the strain rate between 10^{-15} and $10^{-13}\,s^{-1}$.

The rheological parameters A, Q and n depend on the rock type, and therefore have different values for the crust and lithospheric mantle, and for an oceanic and continental plate. As far as the Ionian oceanic slab is concerned, we assume the following rheological parameters for creep. The crust is assumed to be composed of diabase down to 40 km. Ductile strength of diabase is calculated using $A = 2 \times 10^{-4}\,MPa^{-n}\,s^{-1}$, $n = 3.4$, $Q = 260\,kJ\,mol^{-1}$ (Liu and Furlong, 1993). At depths greater than 40 km, the crust is assumed to be eclogitized, due to high pressure–low temperature metamorphism. We assume a mineral composition of eclogite consisting of 60% clinopyroxene and 40% garnet. For this composition we assume the values proposed by Ji and Zhao (1994): $A = 2430\,MPa^{-n}\,s^{-1}$, $n = 2.6$ and $Q = 449\,kJ\,mol^{-1}$. We assume a harzburgitic composition for oceanic lithosperic mantle, and adopt the following parameters: $A = 1010\,MPa^{-n}\,s^{-1}$, $n = 2.4$, $Q = 367\,kJ\,mol^{-1}$ (Ji and Zhao, 1994).

The ductile strength of the crust of the Adriatic continental slab is calculated assuming quartzdiorite rheological parameters down to depths of 40 km: $A = 0.0013\,MPa^{-n}\,s^{-1}$, $n = 2.4$, $Q = 219\,kJ\,mol^{-1}$ (Ranalli, 1997). At depths greater than 40 km, high pressure - low temperature metamorphism is expected to change the mineralogical composition of the crustal portions of subducting continental slabs (e.g., Koons et al., 1987). Following Carminati et al. (2002), we assume that the rheological behavior of HP-LT metamorphosed crust is controlled by quartz and clinopyroxene, with equal volume percentages. The following rheological parameters were calculated by Carminati et al. (2002), using the method of Tullis et al. (1991): $A = 0.00017\,MPa^{-n}\,s^{-1}$, $n = 3.25$, $Q = 248\,kJ\,mol^{-1}$. These parameters are used for the continental crust at depths greater than 40 km. For the dunitic continental lithospheric mantle we assume the following parameters: $A = 2000\,MPa^{-n}\,s^{-1}$, $n = 4$, $Q = 471\,kJ\,mol^{-1}$ (Ranalli, 1997).

We compute at each grid node the brittle and ductile yield stress imposing a posteriori the rheological laws (2) and (3). The differential yield stress required to produce failure is given by the lesser of the brittle and ductile yield stresses (Goetze and Evans, 1979). Nodes with brittle strength lower than ductile strength define the brittle domain, and the opposite stands for the ductile domain.

4.2. Deep earthquake forming mechanisms

We, moreover, discuss the origin of the deep earthquakes in the Ionian slab, under Calabria and the south-

ern Tyrrhenian Sea. The mechanisms originating these earthquakes are most likely different from frictional slip.

Deep focus earthquakes (depths greater than 350 km) have been interpreted as being caused by shear instabilities associated with olivine to spinel transformation and are expected to occur in fast subducting slabs, where metastable olivine wedges can develop (Green et al., 1990; Kirby et al., 1991 and Kirby et al., 1996). Although a quantitative analysis of the rheology of slabs in the mantle transition zone is beyond the scope of this paper, we will investigate if the conditions for the formation of a wedge of metastable olivine are attained.

5. Model results

Fig. 5 shows typical temperature (°C) and lateral anomaly of density (kg m^{-3}) distributions obtained simulating the subduction of an oceanic plate with the TEMSPOL code. In this case, the age of the lithosphere is 120 Myear and the subduction rate 3 cm/year, suitable for the subduction of the Ionian lithosphere under the Calabrian arc. The temperature distribution (Fig. 5a) shows isotherms depressed within the subducting slab. As later widely discussed, lower temperatures in the slab will increase the ductile strength and consequently deepen the brittle-ductile transition with respect to the adjacent mantle. Provided that we assume that the slab penetrates into a static mantle, we are disregarding the effects of possible induced flow in the mantle wedge between the top of the slab and overriding plate. This limitation can lead to significant underestimation of slab-wedge interface temperatures (Van Keken et al., 2002).

We also show in Fig. 5 the location of the olivine-spinel (1% and 99% spinel) transformation. In this case, the 600 °C isotherm, which controls the initiation of metastable olivine to spinel transformation, reaches maximum depths of about 390 km and the conditions for the formation of a small wedge of mestastable olivine are attained. Metastable olivine can persist within the slab down to depths of about 430 km (maximum depth of the 99% spinel curve within the slab), in good agreement with the maximum depth of earthquakes under the southern Tyrrhenian. Deep seismicity is therefore expected to occur for subduction

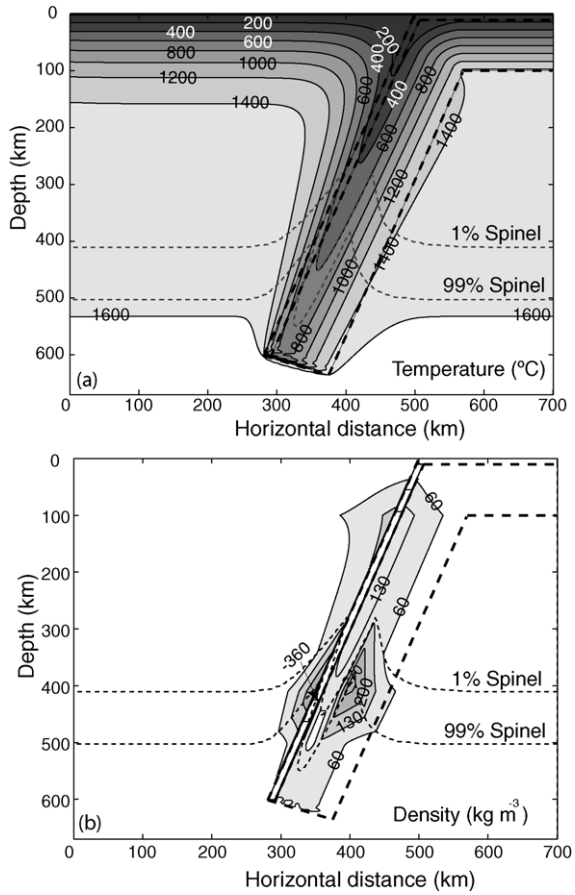

Fig. 5. Temperature (°C) and lateral anomaly of density (with respect to an unperturbed column) (kg m^{-3}) distributions obtained simulating the subduction of an oceanic plate at a rate of 3 cm/year. Note that isotherms (panel a) are depressed in the subducting slab. At a given depth the minimum temperatures are obtained in the internal part of the slab. Density (panel b) increases sharply at the olivine-spinel transition depth.

processes with these kinematic and initial thermal conditions.

The numerical accuracy of temperature calculations was checked by performing a number of convergence tests with systematic variation of grid spacing. Moreover, TEMSPOL code successfully reproduces the results obtained by previous similar thermal models (e.g., Stein and Stein, 1996).

Positive density anomalies (Fig. 5b) in the lithospheric mantle of the slab are due to its lower temperature and to the shallower olivine-spinel transformation within the slab. The density increases sharply at the

olivine-spinel transition depth. It can be inferred from the modelled lateral anomaly of density that slab pull could potentially play a significant role in the present-day geodynamics of the area, in agreement with dynamic numerical models (Giunchi et al., 1996; Negredo et al., 1999). However, this effect could be offset at higher depths by the interaction between the slab and the lower mantle, not included in our modelling. Moreover, the slab pull mechanism is in contrast with the overall down dip compression of the Ionian slab. The small wedge of metastable olivine is characterised by lower densities with respect to the adjacent spinel-bearing mantle. Bina (1996, 1997) proposed, using an elastic rheology for subducting slabs, that the buoyancy associated to the presence of a wedge of metastable olivine could explain the down-dip compression observed within some slabs. Devaux et al. (2000), assuming a viscoelastic rheology, showed that stresses due to buoyancy are negligible compared to internal stresses due to the phase transformation. They obtained, for fast subducting slabs (rates of 10 cm/year), down-dip compression arising from olivine-spinel phase transformation only within the wedge of metastable olivine. Considering the small buoyancy anomalies predicted for the Ionian slab (Fig. 5b) and the small extent of the metastable olivine wedge, the down-dip compression that characterises the slab under the Calabrian arc is hardly linked to such phase transformation. Other mechanisms (for example, slab unbending) should be invoked to explain down-dip compression between 165 and 370 km.

In order to illustrate the influence of the velocity of subduction on the mechanical behaviour of the slab, we display in Fig. 6 the brittle-ductile transition depths obtained for a 120 Myear old oceanic lithosphere subducting at rates of 2, 3 and 4 cm/year (assuming hydrostatic fluid pressure; $\lambda = 0.4$). The sensitivity analysis on the subduction rate is performed on an interval of $\pm 30\%$ of the preferred (3 cm/year) value. This interval is much larger than the 10–15% error on subduction rates inferred from geological and geophysical data. It can be noticed that the brittle-ductile transitions occur at increasing depths for increasing subduction rates. This is readily explained by the fact that faster slabs are colder. Fig. 6 shows that, even without fluid overpressures, the brittle field extends in the modelled oceanic slabs down to depths of 250–320 km. Within the slab, the depth of the olivine-spinel reaction deepens for increasing subduction rates. A small metastable olivine wedge develops only for fast subduction rates (3 and 4 cm/year).

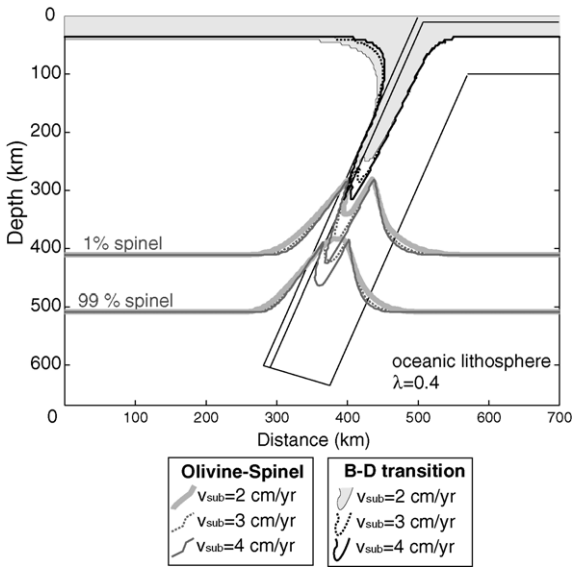

Fig. 6. Brittle-ductile transition depths obtained for 120 Myears old oceanic lithosphere subducting at rates of 2, 3 and 4 cm/year. Notice that the brittle-ductile transitions occur at increasing depth for increasing rates. Within the slab, the depth of the Olivine-Spinel reaction deepens for increasing subduction rates. A small metastable olivine wedge develops only for fast subductions (3 and 4 cm/year).

In order to study the sensitivity of these results to assumed rheological parameters, we have tried different values of the parameters (A, Q and n) used in the ductile yield stress calculations. Typical parameter values for wet and dry olivine give brittle-ductile transitions about 20 and 100 km, respectively, deeper than with the parameters assumed in this study for harzburgite.

In Fig. 7, the effects on brittle-ductile transition depths of fluid pressure and strain rate are investigated. Fig. 7a shows the brittle-ductile transition depths obtained for a 120 Myear old oceanic lithosphere subducting at a rate of 3 cm/year, assuming a constant strain rate of $10^{-13}\,s^{-1}$. The d1-d3 brittle-ductile transition depths are obtained for the three different brittle strength profiles (B1 to B3) shown in Fig. 4. The predicted brittle-ductile transition depths increase from 290 km obtained for no dehydration conditions (B1) to 380 km obtained when considering constant brittle strength at depths greater than 10 km (B3). It should be noted that a drastic increase of fluid pressure (from d1

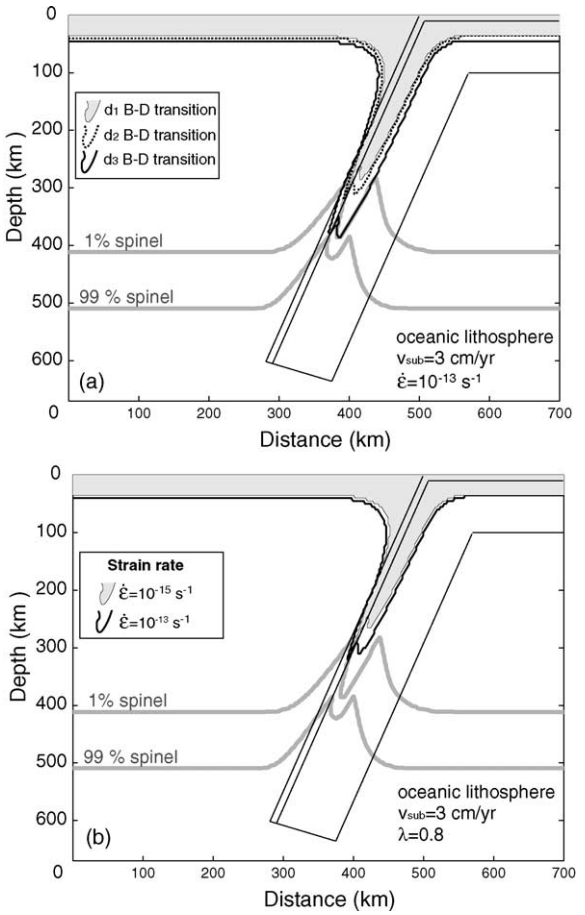

Fig. 7. Brittle-ductile transition depths obtained for 120 Myear old oceanic lithosphere subducting at rates of 3 cm/year. Panel (a) shows the d1–d3 brittle-ductile transition depths obtained for different brittle strength profiles (respectively Sibson's law with $\lambda = 0.4$ and $\lambda = 0.8$ and brittle strength constant at depths greater than 10 km; see Fig. 4 with a constant strain rate of $10^{-13}\,s^{-1}$. Panel (b) shows the influence of strain rate on the brittle-ductile transition depth, with constant $\lambda = 0.8$. Deeper transition depths are predicted for increasing strain rates. Notice that, for an oceanic plate subducting at a rate of 3 cm/year, i.e., similar to the Calabrian slab, a brittle behaviour is predicted at least down to depths ofabout300 km.

to d2) does not dramatically increase the brittle-ductile transition depth. Instead, a down-dip increase of the brittle area of about 70 km occurs between d2 and d3.

As discussed, the reduction of the confining pressure due to dehydration has two effects. First, it reduces the brittle strength so that the shear stress needed for brittle faulting becomes naturally feasible. Second, it increases the depth of the brittle ductile transition, as sketched in Fig. 4. The increase of the brittle-ductile transition depth from d1 to d2 observed in Fig. 7a is small because the ductile yield stress curve is quite horizontal at these depths. On the other hand, dehydration strongly reduces the differential yield stress needed for brittle failure. The fact that an area could potentially behave in a brittle manner without dehydration, does not necessarily imply that it will break or slide frictionally. The required stresses could be too high for brittle faulting to occur. Analogously, the fact that the brittle field has approximately the same extent with or without dehydration does not imply that that brittle faulting will have the same chances to occur in both cases. The far lower differential stresses required in the case of dehydration (three times lower with $\lambda = 0.8$) make brittle faulting more likely when this process is active. Therefore, our study does not neglect the importance of dehydration embrittlement as an earthquake promoting factor.

Fig. 7b shows the influence of strain rate on the brittle-ductile transition depth. In these calculations we assumed $\lambda = 0.8$. Deeper transition depths are predicted for increasing strain rates because ductile yield stress also increases. A brittle behaviour is predicted at least down to depths of about 300 km.

In summary, Figs. 6 and 7 suggest that the intermediate seismicity within the oceanic slab subducting at a rate of 3 cm/year under the Calabrian arc, is compatible with the down-dip extent of the brittle portion of the slab. It is shown that varying extensively the calculation parameters within uncertainty ranges, the brittle-ductile transition depth does not change dramatically. This suggests a good stability of our results.

We have also modelled a subduction process with parameters adequate for the continental subduction of the Adriatic plate under the Northern Apennines (Figs. 8 and 9). Fig. 8 shows the brittle-ductile transition depths obtained for continental lithosphere subducting at a rate of 1 cm/year. A constant $\lambda = 0.8$, a radioactive heat production of $8 \times 10^{-7}\,W\,m^{-3}$, and a strain rate of $10^{-13}\,s^{-1}$ are assumed. The lithospheric thickness is varied between 70 and 120 km, to illustrate the effect of the thermal state of the subducting plate. The predicted brittle-ductile transition depths are much shallower than those predicted for the faster oceanic Ionian slab, in good agreement with the much shallower intermediate-depth seismicity. For a lithospheric thickness of 70 km (adequate for the subducting Adriatic

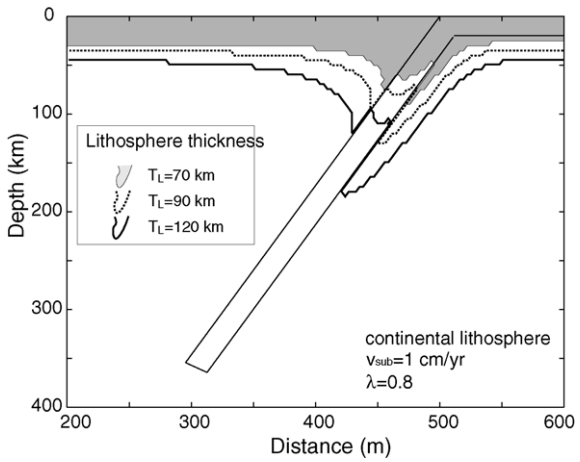

Fig. 8. Brittle-ductile transition depths obtained for continental lithosphere subducting at a rate of 1 cm/year. A constant $\lambda = 0.8$ and a strain rate of $10^{-13}\,s^{-1}$ are assumed. The lithospheric thickness is varied from 70 to 120 km. The plate subducting under the Northern Apennines has a thickness of about 70 km. Only the crustal portion of the slab is shown, since the lithosphere thickness is variable. Note that for a lithospheric thickness of 70 km, the depth of the brittle-ductile transition is predicted at about 100 km, compatibly with earthquake distribution.

plate), the predicted depth of the brittle-ductile transition is of about 100 km, compatibly with earthquake distribution below the Northern Apennines. In other words, the seismogenic portion of the slab is shallower than the real slab extent. Therefore, the maximum depth of earthquakes is not indicative of the maximum depth reached by the Adriatic slab.

With Fig. 9 the effects of fluid pressure and of the brittle strength profile are investigated. These results were obtained for a 70 km thick continental lithosphere subducting at a rate of 1 cm/year. A constant strain rate of $10^{-13}\,s^{-1}$ was assumed. The d1-d3 brittle-ductile transition depths (see Fig. 4 and the above discussion) vary between 70 and 115 km, compatibly with the intermediate-depth seismicity of the area.

It still remain to be investigated whether the different brittle-ductile transition depths predicted for the Ionian and the Adriatic slabs are controlled by temperature distribution (controlled by the subduction rates and thermal state of the subducting plate) or by the different composition (continental vs. oceanic) of the subducting plate. In Fig. 10 we compare with previous results the brittle-ductile transition depth predicted for a subduction process with exactly the same parameters as in Fig. 9 (and $\lambda = 0.8$) but with the rheological parameters *A*, *n* and *Q* used for the oceanic Ionian slab. It can be

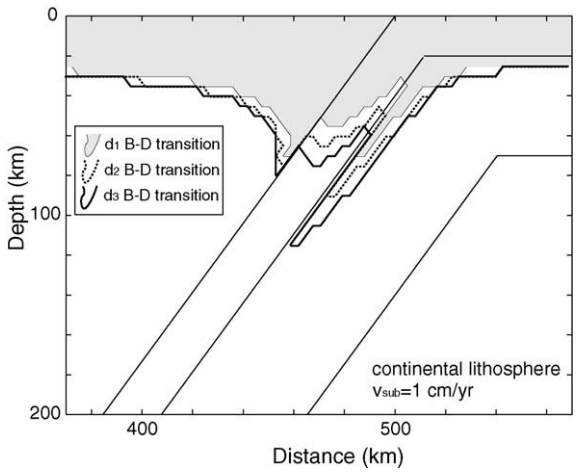

Fig. 9. Brittle-ductile transition depths obtained for a 70 km thick continental lithosphere subducting at a rate of 1 cm/year. A constant strain rate of $10^{-13}\,s^{-1}$ is assumed. The d1-d3 brittle-ductile transition depths are obtained for different brittle strength profiles (respectively Sibson's law with $\lambda = 0.4$ and $\lambda = 0.8$ and brittle strength constant at depths greater than 10 km; see Fig. 3).

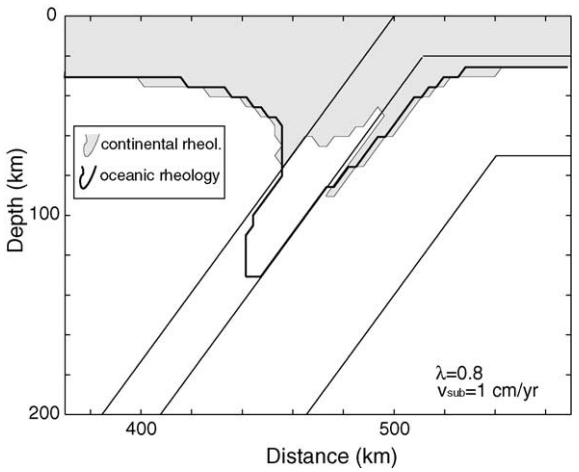

Fig. 10. Brittle-ductile transition depths obtained for a 70 km thick lithosphere subducting at a rate of 1 cm/year. A constant strain rate of $10^{-13}\,s^{-1}$ and $\lambda = 0.8$ are assumed. The two brittle-ductile depths are predicted simulating a continental and an oceanic slab. Notice that, for an oceanic slab, brittle-ductile transition depths are 40 km deeper.

noticed that, for an oceanic slab, the predicted brittle-ductile transition depth is 40 km deeper than for a continental slab. The eclogite composition assumed for the oceanic crust causes a remarkable increase in the depth reached by the brittle portion of the crust, with respect to the continental case. We can deduce from this test that considering an oceanic composition leads to a clear overestimation of the maximum depth of seismicity under the Northern Apennines. The different composition of the subducting plate controls, therefore, the depth of the brittle-ductile transition. The dramatic differences of the intermediate-depth seismicity patterns between the Calabrian and the Northern Apenninic subduction zones are, however, largely due to different thermal distributions within the slab, which are mostly controlled by the increase of subduction rates from north to south.

6. Conclusions

In order to investigate the different patterns of seismicity in the Calabrian and Northern Apennines subduction zones we have modelled the temperature distribution and, assuming a temperature-dependent non-linear rheology, have mapped the brittle and ductile regions of both areas. It is shown that the distribution of the intermediate seismicity zones correlates well with the modelled down-dip extent of the brittle portion for the whole composite Adriatic-Ionian slab. Brittle-ductile transition depths of about 290–380 km and 70–120 km are predicted for the Ionian and Adriatic subduction zones, respectively. This difference is mostly explained by the fact that the Ionian slab, subducting at 3 cm/year rates, is significantly colder than the Adriatic slab, subducting at 1 cm/year rates. The qualitative results obtained do not change assuming different brittle strength profiles, including fluid overpressures caused by dehydration and a constant strength at depths greater than 10 km. The use of fluid overpressures, however, significantly decreases the brittle strength. Dehydration embrittlement, therefore should enhance the occurrence of intermediate seismicity in the Ionian slab. The different nature of the two slabs, being the Ionian slab oceanic and the Adriatic slab continental, also controls the different depth of the brittle-ductile transition.

Concerning deep earthquakes in the Calabrian subduction zone, we have obtained that metastable olivine can persist down to depths of 430 km, in good agreement with the maximum depth of earthquakes in the area. The small extent of the metastable olivine wedge produces a small density anomaly that cannot explain the observed pervasive down-dip compression in the Ionian slab.

Acknowledgements

Spanish research projects Ramón y Cajal, REN2001-3868-C03-02/MAR, and BTE2002-02462 have finantially supported this study. Italian MURST “Progetto Giovani Ricercatori” (E. Carminati) supported this study. Cofin 2001 funding (C. Doglioni) is acknowledged. The thorough reviews of Russ Pysklywec and of an anonymous reviewer and the comments of Peter van Keken greatly improved the manuscript.

References

Akaogi, M., Ito, E., Navrotsky, L., 1989. Olivine-modified spinel-spinel transitions in the system Mg_2SiO_4-Fe_2SiO_4: calorimetric measurements, thermochemical calculation and geophysical application. J. Geophys. Res. 94, 15671–15685.

Amato, A., Selvaggi, G., 1991. Terremoti crostali e sub-crostali nell-Appennino Settentrionale. Studi Geol. Camerti 1, 75–82.

Amato, A., Alessandrini, B., Cimini, G., Frepoli, A., Selvaggi, G., 1993. Active and remnant subducted slabs beneath Italy: evidence from seismic tomography and seismicity. Ann. Geofis. 36, 201–214.

Amato, A., Chiarabba, C., Selvaggi, G., 1997. Crustal and deep seismicity in Italy (30 years after). Ann. Geofis. 40, 981–993.

Anderson, H., Jackson, J., 1987. The deep seismicity of the Tyrrhenian Sea. Geophys. J. R. Astr. Soc. 91, 613–637.

Bally, A.W., Burbi, L., Cooper, C., Ghelardoni, R., 1986. Balanced sections and seismic reflection profiles across the Central Apennines. Mem. Soc. Geol. It. 35, 257–310.

Barberi, F., Gasparini, P., Innocenti, F., Villari, L., 1973. Volcanism of the southern Tyrrhenian sea and its geodynamic implications. J. Geophys. Res. 78, 5221–5232.

Bayer, B., Le Mouel, J.L., Le Pichon, X., 1973. Magetic anomaly pattern in the western Mediterranean. Earth Planet. Sci. Lett. 19, 167–176.

Bigi, G., Cosentino, D., Parotto, M., Sartori, R., Scandone, P., 1990. Structural model of Italy, scale 1:500.000, CNR, Progetto Finalizzato Geodinamica, Firenze.

Biju-Duval, B., et al., 1982. Donnees nouvelles sur les marges du Bassin Ionien profond (Mediterranee Orientale): resultats des campagnes escarmed. Rev. Ist. France Petr., Editions Technip. 37, 713–730.

Bina, C.R., 1996. Phase transition buoyancy contributions to stresses in subducting lithosphere. Geophys. Res. Lett. 23, 3563–3566.

Bina, C.R., 1997. Patterns of deep seismicity reflect buoyancy stresses due to phase transitions. Geophys. Res. Lett. 24, 3301–3304.

Boccaletti, M., Calamita, F., Deiana, G., Gelati, R., Massari, F., Moratti, G., Ricci Lucchi, F., 1990a. Migrating foredeep-thrust belt system in the Northern Apennines and Southern Alps. Palaeogeogr. Palaeoclimatol. Palaeoecol. 77, 3–14.

Boccaletti, M., Ciaranfi, N., Cosentino, D., Deiana, G., Gelati, R., Lentini, F., Massari, F., Moratti, G., Pescatore, T., Ricci Lucchi, F., Tortorici, L., 1990b. Palinspastic restoration and paleogeographic reconstruction of the peri-Tyrrhenian area during the Neogene. Palaeogeogr. Palaeoclimatol. Palaeoecol. 77, 41–50.

Burrus, J., 1984. Contribution to a geodynamic synthesis of the Provencal Basin (Northwestern Mediterranean). Mar. Geol. 55, 247–269.

Byerlee, J.D., 1978. Friction of rocks. Pure Appl. Geophys. 116, 615–626.

Calcagnile, G., Panza, G., 1981. The main characteristics of the lithosphere-asthenosphere system of Italy and surrounding regions. Pure Appl. Geophys. 119, 865–879.

Caputo, M., Panza, G.F., Postpischl, D., 1970. Deep structure of the Mediterranean basin. J. Geophys. Res. 75, 4919–4923.

Carminati, E., Wortel, M.J.R., Spakman, W., Sabadini, R., 1998. The role of slab detachment processes in the opening of the western-central Mediterranean basins: some geological and geophysical evidence. Earth Planet. Sci. Lett. 160, 651–665.

Carminati, E., Giardina, F., Doglioni, C., 2002. Rheological control on subcrustal seismicity in the Apennines subduction (Italy). Geophys. Res. Lett. 29, doi:10.1029.

Catalano, R., Doglioni, C., Merlini, S., 2001. On the Mesozoic Ionian basin. Geophys. J. Int. 144, 49–64.

Della Vedova, B., Pellis, G., 1989. New heat flow density measurements in the Ionian sea. Atti VIII Convegno GNGTS Roma, 1133–1145.

Devaux, J.P., Fleitout, L., Schubert, G., Anderson, C., 2000. Stresses in a subducting slab in the presence of a metastable olivine wedge. J. Geophys. Res. 105, 13365–13373.

de Voogd, B., Truffert, C., Chamot-Rooke, N., Huchon, P., Lallemant, S., Le Pichon, X., 1992. Two-ship deep seismic soundings in the basins of the Eastern Mediterranean Sea (Pasiphae cruise). Geophys. J. Int. 109, 536–552.

Doglioni, C., Fernandez, M., Gueguen, E., Sàbat, F., 1999. On the interference between the early Apennines-Maghrebides backarc extension and the Alps-Betics orogen in the Neogene Geodynamics of the Western Mediterranean. Boll. Soc. Geol. It. 118, 75–89.

Fernandez, M., Ranalli, G., 1997. The role of rheology in extensional basin formation modelling. Tectonophysics 282, 129–145.

Frepoli, A., Selvaggi, G., Chiarabba, C., Amato, A., 1996. State of stress in the southern Tyrrhenian subduction zone from fault plane solutions. Geophys. J. Int. 125, 879–891.

Giardini, D., Velonà, M., 1991. The deep seismicity of the Tyrrhenian Sea. Terra Nova 3, 57–64.

Giunchi, C., Sabadini, R., Boschi, E., Gasperini, P., 1996. Dynamic models of subduction: geophysical and geological evidence in the Tyrrhenian Sea. Geophys. J. Int. 126, 555–578.

Goetze, C., Evans, B., 1979. Stress and temperature in the bending lithosphere as constrained by experimental rock mechanics. Geophys. J. R. Astron. Soc. 59, 463–478.

Green, H.W., Young, T.E., Walker, D., Scholz, C.H., 1990. Anticrack-associated faulting at very high pressure in natural olivine. Nature 348, 720–722.

Green, H.W., 1994. Solving the paradox of deep earthquakes. Sci. Am. 271, 64–71.

Gueguen, E., Doglioni, C., Fernandez, M., 1998. On the post 25 Ma geodynamic evolution of the western Mediterranean. Tectonophysics 298, 259–269.

Hacker, B.R., Peacock, S.M., Abers, G.A., Holloway, S.D., 2003. Subduction factory 2. Are intermediate-depth earthquakes in subducting slabs linked to metamorphic dehydration reactions? J. Geophys. Res. 108 (B1), doi: 10.1029/2001JB001129.

Hobbs, B.E., Ord, A., 1988. Plastic instabilities: Implications for the origin of intermediate and deep focus earthquakes. J. Geopgys. Res. 93 (10), 521–610, 540.

Isacks, B., Molnar, P., 1971. Distribution of stresses in the descending lithosphere from a global survey of focal-mechanism solutions of mantle earthquakes. Rev. Geophys. Space Phys. 9, 103–174.

Jaeger, J.C., Cook, N.G.W., 1979. Fundamentals of Rock Mechanics, third edition. Mathuen, London, p. 593.

Jeffreys, H., 1929. The Earth, its origin history and physical constitution. Cambridge University Press.

Ji, S., Zhao, P., 1994. Layered rheological structure of subducting oceanic lithosphere. Earth Planet. Sci. Lett. 124, 75–94.

Kirby, S.H., Durham, W.B., Stern, L.A., 1991. Mantle phase changes and deep-earthquake faulting in subducting lithosphere. Science 252, 216–225.

Kirby, S.H., Stein, S., Okal, E., Rubie, D.C., 1996. Metastable mantle phase transformations and deep earthquakes in subducting oceanic lithosphere. Rev. Geophys. 34, 261–306.

Koons, P.O., Rubie, D.C., Frueh-Green, G., 1987. The effects of disequilibrium and deformation on the mineralogical evolution of Quarts Diorite during metamorphism in the eclogite facies. J. Petrol. 28, 679–700.

Liu, M., Furlong, K., 1993. Crustal shortening and Eocene extension in the southeastern Canadian Cordillera; some thermal and rheological considerations. Tectonics 12, 776–786.

Lucente, F.P., Chiarabba, C., Cimini, G.B., Giardini, D., 1999. Tomographic constraints on the geodynamic evolution of the Italian region. J. Geophys. Res. 104, 20307–20327.

Malinverno, A., Ryan, W.B.F., 1986. Extension in the Tyrrhenian Sea and shortening in the Apennines as result of arc migration driven by sinking of the lithosphere. Tectonics 5, 227–245.

Meade, C., Jeanloz, R., 1991. Deep-focus earthquakes and recycling of water into the Earth's mantle. Science 252, 68–72.

Minear, J.W., Toksöz, M.N., 1970. Thermal regime of a downgoing slab and new global tectonics. J. Geophys. Res. 75 (1), 397–401, 419.

Negredo, A.M., Sabadini, R., Bianco, G., Fernandez, M., 1999. Three-dimensional modelling of crustal motions caused by sub-

duction and continental convergence in the central Mediterranean. Geophys. J. Int. 136, 261–274.

Negredo, A.M., Valera, J.L., Carminati, E., 2004. TEMSPOL: a MATLAB thermal model for deep subduction zones including major phase transformations. Comput. Geosci. 30, 249–258.

Ogawa, M., 1987. Shear instability in a viscoelastic material as the cause of deep focus earthquakes. J. Geophys. Res. 92 (13), 801–813, 810.

Patacca, E., Scandone, P., 1989. Post-Tortonian mountain building in the Apennines. The role of the passive sinking of a relic lithospheric slab. In: Boriani, A., Bonafede, M., Piccardo, G.B., Vai, G.B. (Eds.), In: The Lithosphere in Italy, Accad. Naz. Lincei., vol. 80, pp. 157–176.

Piromallo, C., Morelli, A., 1998. P-wave propagation heterogeneity and earthquake location in the Mediterranean region. Geophys. J. Int. 135, 232–254.

Piromallo, C., Morelli, A., 2002. P-wave tomography of the mantle under the Alpine-Mediterranean area. J. Geophys. Res., doi: 10.1029/2002JB001757.

Raleigh, C.B., Paterson, M.S., 1965. Experimental deformation of serpentinite and its tectonic implications. J. Geophys. Res. 70, 3965–3985.

Ranalli, G., 1997. Rheology and deep tectonics. Ann. Geofis. 40, 671–680.

Ricci Lucchi, F., 1986. The oligocene to recent foreland basins of the Northern Apennines. In: Allen, P.A., Homewood, P. (Eds.), Foreland Basins, Spec. Publ. Intern. Ass. Sedim., vol. 8, pp. 105–140.

Rubie, D.C., Ross, C.R., 1994. Kinetics of the olivine-spinel transformation in subducting lithosphere: experimental constraints and implications for deep slab process. Phys. Earth Planet. Interiors 86, 223–241.

Schmeling, H., Monz, R., Rubie, D.C., 1999. The influence of olivine metastability on the dynamics of subduction. Earth Planet. Sci. Lett. 165, 55–66.

Serri, G., Innocenti, F., Manetti, P., 1993. Geochemical and petrological evidence of the subduction of delaminated Adriatic continental lithosphere in the genesis of the Neogene—Quaternary magmatism of central Italy. Tectonophysics 223, 117–147.

Shimada, M., 1993. Lithosphere strength inferred from fracture strength of rocks at high confining pressures and temperature. Tectonophysics 217, 55–64.

Sibson, R.H., 1981. Controls on low-stress hydro-fracture dilatancy in thrust, wrench and normal fault terrains. Nature 289, 665–667.

Spakman, W., van der Lee, S., van der Hilst, R., 1993. Travel-time tomography of the European-Mediterranean mantle down to 1400 km. Phys. Earth Planet. Int. 79, 3–74.

Stein, C.A., Stein, S., 1992. A model for the global variation in oceanic depth and heat flow with lithospheric age. Nature 359, 123–129.

Stein, S., Stein, C.A., 1996. Thermo-mechanical evolution of oceanic lithosphere: implications for the subduction process and deep earthquakes. Subduction from top to bottom. Geophys. Monogr. 95, 1–17.

Tullis, T.E., Horowitz, F.G., Tullis, J., 1991. Flow laws of poliphase aggregates from end member ow laws. J. Geophys. Res. 96, 8081–8096.

Turcotte, D.L., Schubert, G., 2002. Geodynamics, vol. 456, second edition Cambridge University Press, Cambridge, UK, p. 456.

Vai, G.B., 1989. Migrazione complessa del sistema deformativo-avanfossa-cercine periferico: il caso dell'Appennino settentrionale. Mem. Soc. Geol. It. 38, 95–105.

Van Keken, P.E., Kiefer, B., Peacock, S.M., 2002. High-resolution models of subduction zones: Implications for mineral dehydration reactions and the transport of water into the deep mantle. G3, 1056. doi:10.1029/2001GC000256.

Yamasaki, T., Seno, T., 2003. Double seismic zone and dehydration embrittlement of the subducting slab. J. Geophys. Res. 108 (B4), doi:10.1029/2002JB001918.

Wang, K., 2002. Unbending combined with dehydration embrittlement as a cause for double and triple seismic zones. Geophys. Res. Lett. 18, doi:10.1029/2002GL015441.